

## THE DESIGN OF EDFA WITH FORWARD PUMPING AT THE DISTANCE LINE IN DWDM

PETR IVANIGA<sup>1,\*</sup>, TOMAŠ IVANIGA<sup>2</sup>

<sup>1</sup>Department of Information Networks Faculty of Management Science and Informatics, University of Žilina, Žilina, Slovakia

<sup>2</sup>Department of Electronics and Multimedia Communications, Faculty of Electrical Engineering and Informatics, University of Technology Košice, Košice, Slovakia

\*Corresponding Author: petr.ivaniga@fri.uniza.sk

### Abstract

The aim of this article is the design of a suitable EDFA amplifier with forward pumping ready to be implemented into an 8-channel DWDM system (ITU-T G-694.1) to manage a distance of 3000 km. The mentioned amplifier is placed IN-LINE in the optical loop and it is amplified in C-band (1530-1565 nm). The optical loop is created from optical fibre with a length of 95 km and with an increment of 5 (475 km). The article shows a decrease in the Q-factor when the bit speed and distance increase. The system has been designed to manage distance with a constant bit speed with the length of the erbium-doped fibre of 14 m. The channel gap was set to the value of 50GHz due to FWM while the system regards SPM and CPM.

Keywords: ASE, BER, EDFA, Forward pumping, Q-factor.

## 1. Introduction

For illustration purposes let us suppose the  $\text{Er}^{3+}$  ions doping the environment can exist in at least two discreet states, excited and ground. The number of ions in the individual energy levels are set by the Boltzmann distribution in thermal balance conditions [1, 2]. The majority of ions are in the ground state with minimal energy. Albert Einstein theoretically explained the interaction of such a group of ions using quantum of light energy - photons [3-5]. It talks about three different effects that can possibly occur: absorption, stimulated emission and spontaneous emission [6, 7]. The absorption of a photon with energy equal to the difference between the energy levels leads the ion in the ground state into the excited state.

From the excited meta-stable state the ion returns to the ground state either spontaneously (concurrently with the photon radiation with the accidental polarisation and phase) or it is stimulated to the photon emission by another photon. In the case of stimulated emission both photons have the identical polarisation and phase properties. They are coherent [8, 9]. An active environment's thermal balance can be distressed for example by the presence of a pumping light source [10-13]. If the other influence is absent in the active environment, most of the ions stay in the excited state permanently. In the case of the optical signal being inducted into the excited state of the active environment, the photons of the optical signal will gravitate more towards stimulated emission than absorption and so the signal will be amplified [14-16]. The photons generated by the spontaneous emission contribute towards the increase of the amplifier noise.

The ions of Erbium (as the member of the lanthanide group of rare earths) the excited transitions happen between energy levels on the energy level  $4f$ . The electron configuration of lanthanides is  $[\text{Xe}] 4f^{N-1}.5s^2.5p^6.6s^0$ , where  $[\text{Xe}]$  represents the closed level configuration of Xenon [16-18]. In this ion configuration there is one electron taken from the level  $4f$  and two from  $6s$ , according to the energy availability in which the electrons occupy the energy levels. On the other side  $N-1$  of the inner electrons the levels  $4f$  remain sheltered from the outer fields by the outer levels  $5s$  and  $5p$ , so  $4f \rightarrow 4f$  laser transitions show relatively sharp spectral lines [19, 20]. The other consequence is lessened sensitivity of the spectral properties of the  $4f \rightarrow 4f$  transition to the host material type. Even this small influence caused by the host material is important for the laser applications. For the ion  $\text{Er}^{3+}$  is true  $N = 12$ . In its layer it has  $4f N-1=11$  electrons, which can acquire a total of 14 various energy levels. These levels are discreet and linear in the case of  $\text{Er}^{3+}$ , ion placed in the vacuum. But should the ion be built into, for example, a glass matrix of the optical fibre, the line levels widen into strips. The energy levels with the importance of the signal amplification in band 1500nm are displayed in Fig. 1a. On Fig. 1b is the meta-stable level  ${}^4I_{13/2}$ , which can utilised directly on 1480nm or through the level  ${}^4I_{11/2}$  on 980nm [21-23]. The lifespan of the ion on the level  ${}^4I_{11/2}$  is very short compared with the lifespan of the level  ${}^4I_{13/2}$ . The ion excited to the level  ${}^4I_{11/2}$  will transition into the meta-stable level  ${}^4I_{13/2}$ . This levels are marked according to the "Russell-Saunders" coupling convention with its origin in the quantum atomic theory (Fig.1) [1]. On Fig. 1b is the levels' expansion shown on the shape of the absorption and the emission spectre of the transition  ${}^4I_{15/2} \leftrightarrow {}^4I_{13/2}$  in the Erbium-doped optical fibre.

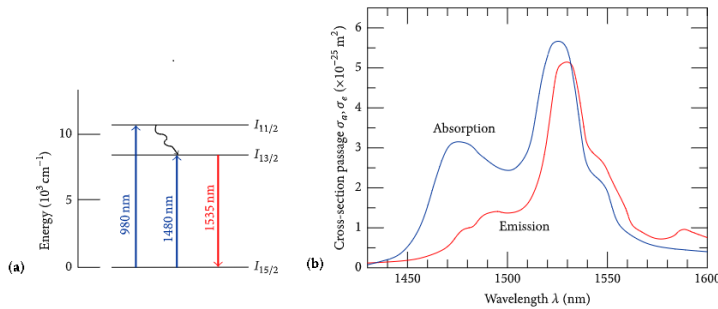


Fig. 1. Visualisation of the energy levels and the meta-stable level.

## 2. Bit Error Rate

Bit Error Ratio BER is another characteristic, very useful for finding out a system performance. BER parameter describes the ratio between bits wrongly detected and a total number of bits received (transmitted). The information is detected in two levels, “0” and “1”. These two levels have corresponded with current values  $I_1, I_2$  as well as their variances  $\sigma_1, \sigma_2$ . The variances have usually different values [24, 25]. If the incoming signal has a value within  $\sigma_1, I_1$  region “1” is detected, the analogical process is applied with “0” level detection. However, sometimes system makes an error and “0” is recognized when “1” was transmitted to  $P(0/1)$  (a lower region). Complementary “1” can be detected when “0” was sent to  $P(1/0)$  (an upper region). Corresponding probability functions are defined as follows

$$P(0/1) = \frac{1}{\sqrt{2\pi}\sigma_1} \int_{-\infty}^{I_{th}} e^{-\frac{(I-I_1)^2}{2\sigma_1^2}} dI, \quad (1)$$

$$P(1/0) = \frac{1}{\sqrt{2\pi}\sigma_0} \int_{I_{th}}^{\infty} e^{-\frac{(I-I_0)^2}{2\sigma_0^2}} dI, \quad (2)$$

The next step is to define some complementary error functions for  $P(0/1)$  and  $P(1/0)$

$$P(0/1) = \frac{1}{2} \operatorname{erfc} \left( \frac{I_1 - I_{th}}{\sigma_1 \sqrt{2}} \right), \quad (3)$$

$$P(1/0) = \frac{1}{2} \operatorname{erfc} \left( \frac{I_{th} - I_0}{\sigma_0 \sqrt{2}} \right). \quad (4)$$

Based on studies by Ivaniga and Ivaniga [7], BER has the minimum value when  $P(0/1)$  and  $P(1/0)$  regions are equal. From this assumption, we have to set the following condition for a threshold current  $I_{th}$ , which is important to be set correctly

$$\frac{I_1 - I_{th}}{\sigma_1} = \frac{I_{th} - I_0}{\sigma_0} \Rightarrow I_{th} = \frac{\sigma_0 I_1 + \sigma_1 I_0}{\sigma_1 + \sigma_0}. \quad (5)$$

Now we can define another parameter called Q-factor

$$Q = \frac{I_1 - I_0}{\sigma_1 + \sigma_0} . \quad (6)$$

Q-factor describes the margin between two levels, “0” and “1”, and their relation to the corresponding variances  $\sigma_1, \sigma_2$  [3, 7]. By assuming that BER is a sum of the regions shown in Eqs. (3) and (4), we can define the following Eq. (7)

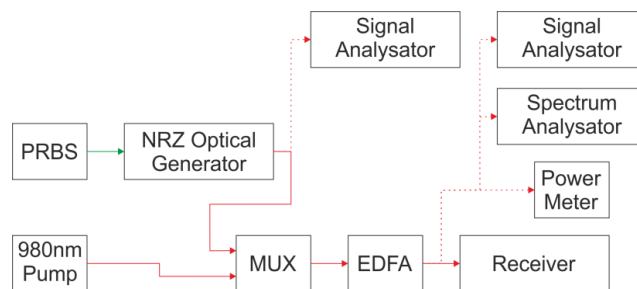
$$BER = \frac{1}{4} \left\{ \operatorname{erfc} \left( \frac{I_1 - I_{th}}{\sigma_1 \sqrt{2}} \right) + \operatorname{erfc} \left( \frac{I_{th} - I_0}{\sigma_0 \sqrt{2}} \right) \right\} . \quad (7)$$

Now it is possible to write a final equation for BER as well as its approximation by using the exponential function as shown in the following equation

$$BER = \frac{1}{2} \operatorname{erfc} \left( \frac{Q}{\sqrt{2}} \right) \approx e^{-\frac{Q^2}{2}} / Q\sqrt{2\pi} . \quad (8)$$

### 3. Design of the EDFA Connection with the Appropriate Modification Pump-power

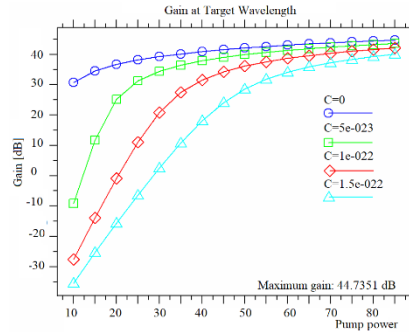
The whole first experimental system contains 5 basic parts, which are subsequently implemented into DWDM system (Fig. 2). The data source (PRBS) has a set transfer speed of 12.5 Gbps, with its logic signal entering the optical generator. The generator used the NRZ coding and the filter of the “Ring” type. The generated optical signal enters the multiplexor and then the amplifier. Simulations were performed for the connections with co-propagating, counter-propagating and bidirectional pumping - with the forward pumping insufficiently lagging. The whole system is amplified in C-band for the wavelength 1550 nm. The forward pump is set to 980 nm with power of 60 mW. In such connection, there was an iteration created in order to compare gain, noise figure NF and spontaneous emission ASE. In the whole iteration, the pumping power is changed from 10 mW to 85 mW with the increment 5 and subsequently the  $k$  value with the increment 0.1 from the value 0 to 0.3 (Fig. 3).



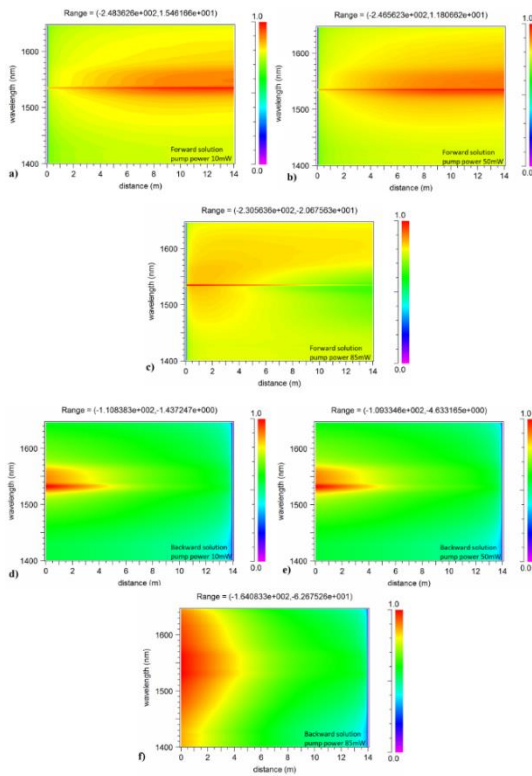
**Fig. 2. Experimental model for the EDFA connection with forward pumping.**

Figure 3 shows the maximal gain for the value of  $k = 0$  and it shows the increase of  $k$  value resulting in the decrease of EDFA gain. From these graphs, the maximal gain equals the value of 44.7531 dB and NF equals 3.25729.

ASE is the noise or basically the light created by spontaneous emission, optically amplified by the process of the stimulated emission within the fibre. ASE influences the maximal achievable gain negatively. On Figs. 4(a)-(d) can be observed the forward solution and the backward solution with changes in the pump-power (10 mW, 50 mW, 85 mW). The whole system will notice the decrease in Q-factor and the increase in BER in its output due to ASE.



**Fig. 3. Change of the pump-power for EDFA to gain at 1550 nm for  $k=0, k=0.1, k=0.2, k=0.3$ .**



**Fig. 4. (a) Backward solution-10 mW, (b) Backward solution-50 mW, (c) Backward solution-85 mW, (d) Forward solution-10 mW, (e) Forward solution-50 mW, (f) Forward solution-85 mW.**

The key component of EDFA is the constant length of the Erbium-doped fibre during all simulations (14 m) and the fiber saturation parameter set to  $3.10^{15} \text{ m}^{-1}\text{s}^{-1}$ . In Fig. 5, the change of the pumping power to the change of the length of the optical fibre is shown. The iteration was formed where the pumping power changes from 20 mW to 85 mW to the length of Erbium-doped fibre from 2 m to 20 m, with the increment of 1 m. With the pumping power of 35 mW the optical power was -5.7233 dBm. At 50 mW the power changed to 2.5419 dBm, at 65 mW this was 3.9082 dBm and at 80 mW the optical power equalled 4.9511 dBm. According to the results from this graph the length of the Erbium-doped fibre was chosen. The spectral model of a 980 nm is of the “rectangular” type, the loss is 6.2 dB/m and the width is set to 20 nm. The EDFA connection is without mirrors.

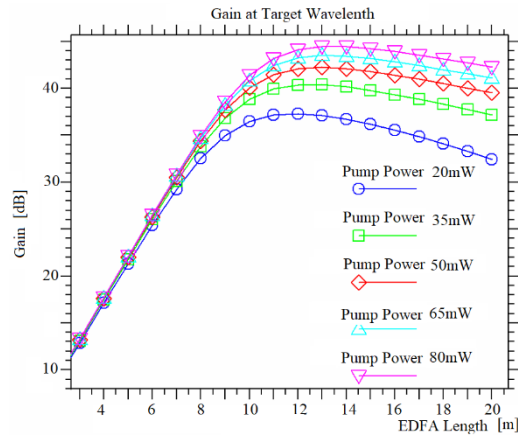


Fig. 5. Change of Erbium-doped fibre to change in the pump power.

### 3.1. Necessity of using EDFA as the IN-LINE amplifier

For the purpose of the graph line's evaluation the system will be evaluated based on its Q-factor for the respective wavelength. Mathematical calculation of BER and its corresponding Q-factor is described in chapter 2. Figure 6 contains the graph of creating the optical loop using EDFA. Figure 6 shows the changing bit speed from 10 Gbps-40 Gbps with the increment of 10 Gbps for lengths of fibre 80 km-160 km with the increment of 10 km and the corresponding Q-factor. From the results, it is clear that the increasing bit speed means a fall in Q-factor. For 10 Gbps without the use of EDFA the Q-factor equalled 7.6869, for 20 Gbps it equalled 3.2794, at 30 Gbps it equalled 1.6958 and at 40 Gbps it equalled 1.0198. In Fig. 2, the whole created system is without the use of the optical loop. This system will be expanded with optical transmitters and the optical loop in order to reach the maximal distance with EDFA connected. Our system was designed for 12.5 Gbps with the corresponding Q-factor of 5.9779 with the length of the optical fibre 95 km.

The quality of the optical line is considered acceptable with Q-factor of approximately 6 and with BER of about  $10^{-11}$  and less.

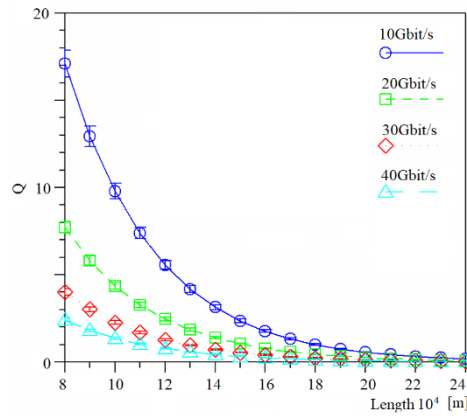


Fig. 6. Relationship of the Q-factor to distance with changed bit speed.

### 3.2. Practical design of DWDM with the optical loop

The 8-channel DWDM system was formed with gaps of 50 GHz between the respective channels (Fig. 7). Every transmitting part is expanded by CW with the power of 1 mW and by an external modulator using the modulation of the “MachZehnder” type. The individual optical signals enter the multiplex where they merge. The resulting optical signal enters the created optical loop for the purpose of travelling the maximal distance.

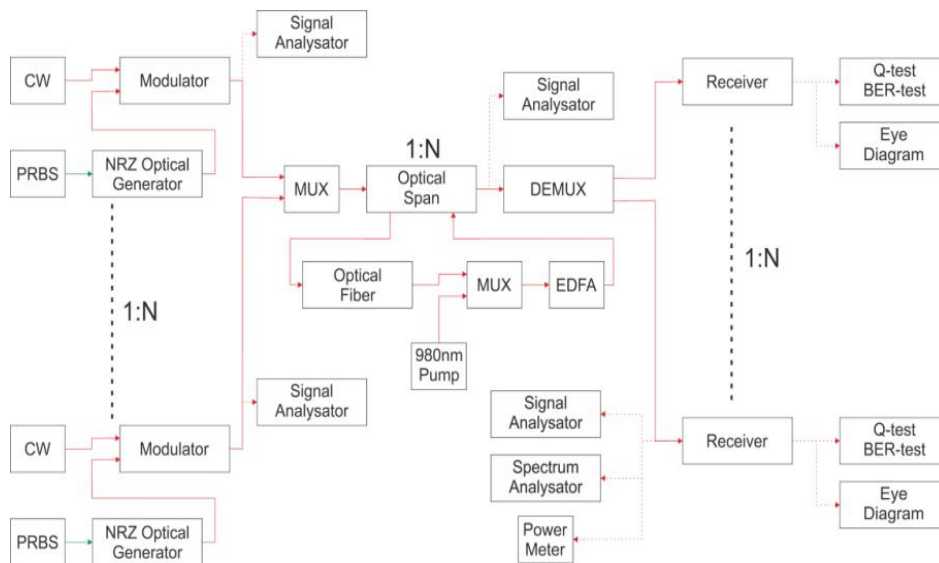


Fig. 7. Design of the DWDM system according to ITU-T G.694.1.

We compared the Q-factor for the wavelength of 1550 nm in our topology. In the optical loop, a non-linear optical fibre 95 kms long was used. Total loss for this fibre was 0.33 dB.km<sup>-1</sup>.  $\lambda_0$  is 1312 nm and  $n_1$  is set to 1.4682 with a diameter of 8 $\mu$ m and the fibre included the effects SPM and CPM. However, neither SBS, PMD nor the

Raman effect were considered during the simulations. Presentation of the final results was based on the "Monte-Carlo" method and using the "Bessel" filter.

With bit speed of 12.5 Gbps for the distance of 1900 km Q was 11.22. According to Fig. 6 Q will decrease with the increasing distance. At 2375 km Q fell to 8.8982 with the value of BER  $2.8388 \cdot 10^{-19}$ . The system is designed to manage the maximal distance and not cross the minimal value when Q equals approximately 6. Because the optical loop was created with the increment 5, all the simulations are with the gap of 475 km. For 2850 km Q equals 7.3113 with BER  $1.3230 \cdot 10^{-13}$ . For 3325 km Q equals 6.0095, which represents the minimal value for the quality transfer in the optical fibre. For 3800 km Q reached the value of 4.9252 for BER  $4.2136 \cdot 10^{-7}$ , which is insufficient. The system designed by us with the given EDFA parameters can manage a distance of 3325 km (Fig.8).

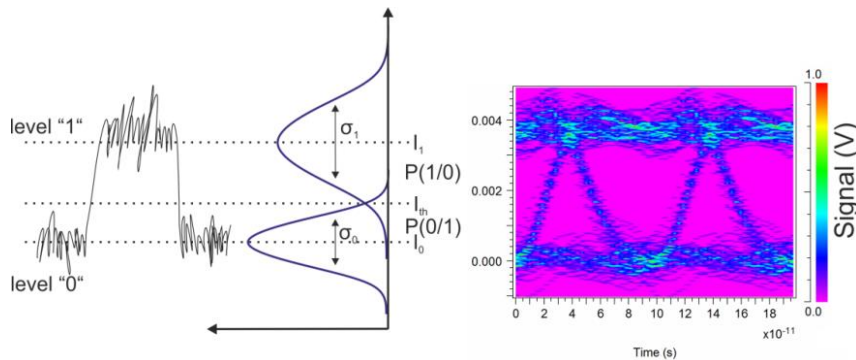


Fig. 8. Final BER at the output after 3325 km.

#### 4. Conclusion

The aim of this article was the practical design of EDFA in the optical loop. The article shows the appropriate setting of the pump-power in EDFA and the appropriate choice of the length of the Erbium-doped fibre for the most gain-profitable purpose (in this case it is 14 m length). The subsequent implementation of EDFA into the optical loop shows the system's practical design for long distance lines. It evaluates the system based on its Q-factor. The main contribution of this article is the length of the optical fibre 95 kms in the optical loop to manage 3325 km in a DWDM system ( $Q = 6.0095$ , BER= $5.6213 \cdot 10^{-10}$ ). The IN-LINE placement of EDFA is essential in designing fully optical communication systems. The design in addition encompasses the non-linear effects, such as SPM, FWM or CPM, connected with the power and gapping of/in the optical lines.

#### Nomenclatures

$Er^{3+}$	Erbium Ion
$^4I_{11/2}$	Meta-stable level
$^4I_{13/2}$	Meta-stable level
$^4I_{15/2}$	Meta-stable level
$XE$	Xenon

**Abbreviations**

ASE	Amplified Spontaneous Emission
BER	Bit Error Rate
CWDM	Coarse Wavelength Division Multiplex
CPM	Cross Phase Modulation
DWDM	Dense Wavelength Division Multiplex
EDFA	Erbium Doped fiber Amplifier
FWM	Four Wave Mixing
MUX	Multiplexor
NF	Noise Figure
NRZ	Non Return To Zero
SPM	Self-Phase Modulation

**References**

1. Ivaniga, T.; and Ivaniga, P. (2017). Comparison of the optical amplifiers EDFA and SOA based on the BER and Q-factor in C-band. *Advances in Optical Technologies*, Article ID 9053582, 9 pages.
2. Ivaniga, P.; and Ivaniga, T. (2017). 10 Gbps optical line using EDFA for long distance lines. *Przeglad Elektrotechniczny*, 93(3), 193-196.
3. Mikus, L. (2010). Evaluations of the error rate in backbone networks. *Elektrorevue*, 12(2), 1-6. (in Czech).
4. Smiesko, J.; and Uramova J. (2012). Access node dimensioning for IPTV traffic using effective bandwidth. *Communications*, 14(2), 11-16.
5. Bosternak Z.; and Roka, R. (2018). Bandwidth scheduling methods for the upstream traffic in passive optical networks. *Przeglad Elektrotechniczny*, 94(4), 9-12.
6. Papan, J.; Segec, P.; Drozdova, M.; Mikus, L.; Moravcik, M.; and Hrabovsky, J. (2016). The IPFRR mechanism inspired by BIER algorithm. *Proceedings of the International Conference on Emerging eLearning Technologies and Applications (ICETA)*. Vysoke Tatry, Slovakia, 257-262.
7. Ivaniga, P.; and Ivaniga, T. (2017). Comparison of DPSK and RZ-DPSK modulations in optical channel with speed of 10 Gbps. *Journal of Information and Organizational Sciences*, 41(2), 185-196.
8. Smiesko, J. (2003). Exponential model of token bucket system. *Komunikacie*, 4, 66-70.
9. Toth, J.; Ovsenik, L.; and Turan, J. (2015). An overview of various types of waveguide grating based demultiplexors in WDM systems. *Proceedings of the International Conference on Systems, Signals and Image Processing (IWSSIP)*. London, United Kingdom, 29-32.
10. Mikus, L. (2003). Available tools for the educational course development. *Proceedings of the 2<sup>nd</sup> International Conference on Emerging Telecommunications Technologies*. Kosice, Slovakia, 295-297.
11. Bachrata, K. (2003). Effective bandwidth for deterministic networks. *Komunikacie*, 4, 78-82.

12. Abdullaev, A.; and Turan, J. (2014). Survey of the problems and solutions of arrayed waveguide gratings used in the optical networks. *Acta Electrotechnica et Informatica*, 14(3), 49-53.
13. Skorpil, V.; and Precechtel, R. (2013). Training a neural network for a new node element design. *Przegląd Elektrotechniczny*, 89(2B), 187-192.
14. Pinosova, M.; Andejiova, M.; Liptai, P.; and Lumintzer, E. (2018). Objective and subjective evaluation of the risk physical factors near to conveyor system. *Advances in Science and Technology Research Journal*, 12(3), 188-196.
15. Steingartner, W.; and Novitzka, V. (2016). Categorical model of structural operational semantics for imperative language. *Journal of Information and Organizational Sciences*, 40(2), 203-219.
16. Ruzbarsky, J.; Turan, J.; and Ovsenik, L. (2016). Stimulated brillouin scattering in DWDM all optical communication systems. *Proceedings of the 26<sup>th</sup> International Conference on Radioelektronika*. Kosice, Slovakia, 395-398.
17. Kheraliya, S.; and Kumar, C. (2018). Comparative study of various optical amplifiers for 32-channel WDM system. *Journal of Optical Communications*, 1-9.
18. Mukherjee, P.P.; Sarkar, S.; and Das, N.R. (2013). A comparative study on determination of optimum detection threshold for minimum BER in a WDM receiver with component crosstalk. *Proceedings of the International Conference on Microwave and Photonics (ICMAP)*. Dhanbad, India, 1-4.
19. Klimo, M.; Bachrata K.; Smiesko, J.; Uramova, J.; and Cenek, P. (2009). *Theory of IP telephony*, 379.
20. Hakim, M.A.; and Sathi, Z.M. (2017). Modified square lattice photonic crystal fiber (SLPCF) incorporating EDFA and definite power CW laser for improved RoF link. *Proceedings of the 2<sup>nd</sup> International Conference on Electrical & Electronic Engineering (ICEEE)*. Rajshahi, Bangladesh, 1-4.
21. Marton, M.; Ovsenik, L.; Turan, J.; Spes, M.; and Vasarhelyi, J. (2018). Possibility of increasing availability of FSO/RF hybrid system with implementation of helix antenna for 5.2 GHz. *Proceedings of the 19<sup>th</sup> International Carpathian Control Conference (ICCC)*. Szilvasvarad, Hungary, 498-501.
22. Raghuwanshi, S.K.; and Sharma, R. (2015). Modeling of forward pump EDFA under pump power through MATLAB. *International Nano Letters*, 5(3), 155-160.
23. Huszanik, T.; Turan, J.; and Ovsenik, L. (2018). Comparative analysis of optical IQ modulation in four-channel DWDM system in the presence of fiber nonlinearities. *Proceedings of the 19<sup>th</sup> International Carpathian Control Conference (ICCC)*. Szilvasvarad, Hungary, 468-473.
24. Huszanik, T.; Turan, J.; and Ovsenik, L. (2018). Demonstration of multimode optical fiber communication system using 1300 nm directly modulated VCSEL for gigabit Ethernet. *Infocommunications Journal*, 10(2), 26-32.
25. Tarjanyi, N.; and Kacik, D. (2017). Lithium niobate-based integrated photonics utilizing photorefractive effect. *Communications*, 19(3), 77-82.